J Biomol NMR (2014) 59:199–210
DOI 10.1007/s10858-014-9839-x

ARTICLE

A reduced dimensionality NMR pulse sequence and an efficient protocol for unambiguous assignment in intrinsically disordered proteins

Jithender G. Reddy · Ramakrishna V. Hosur

Received: 25 January 2014 / Accepted: 8 May 2014 / Published online: 23 May 2014

Abstract Resonance assignment in intrinsically disordered proteins poses a great challenge because of poor chemical shift dispersion in most of the nuclei that are commonly monitored. Reduced dimensionality (RD) experiments where more than one nuclei are co-evolved simultaneously along one of the time axes of a multi-dimensional NMR experiment help to resolve this problem partially, and one can conceive of different combinations of nuclei for co-evolution depending upon the magnetization transfer pathways and the desired information content in the spectrum. Here, we present a RD experiment, (4,3)D-hNCOCAnH, which uses a combination of CO and CA chemical shifts along one of the axes of the 3-dimensional spectrum, to improve spectral dispersion on one hand, and provide information on four backbone atoms of every residue—HN, N, CA and CO chemical shifts—from a single experiment, on the other. The experiment provides multiple unidirectional sequential ($i \rightarrow i - 1$) amide ^{1}H correlations along different planes of the spectrum enabling easy assignment of most nuclei along the protein backbone. Occasional ambiguities that may arise due to degeneracy of amide proton chemical shifts are proposed to be resolved using the HNN experiment described previously (Panchal et al. in J Biomol NMR 20:135–147, 2001). Applications of the experiment and the assignment protocol have been demonstrated using intrinsically disordered α-synuclein (140 aa) protein.

Keywords Multidimensional NMR spectroscopy · Intrinsically disordered proteins · ^{13}C/^{15}N-doubly labeled proteins · Reduced dimensionality · Backbone resonance assignment · Check points

Introduction

Despite commendable developments in NMR methodologies during the past two decades time-efficient and unambiguous assignment of backbone resonances in intrinsically disordered proteins has remained problematic and challenging due to high degree of backbone amide and carbon shift degeneracy in such proteins (Dyson and Wright 2001, 2004; Eliezer 2006; Permi and Hellman 2012; Felli and Pierattelli 2012; Kosol et al. 2013; Kragelj et al. 2013). The difficulties get compounded when there are amino-acid repeats in a particular stretch or when there are particular stretches of amino acids repeating along the sequence. A number of multi-dimensional NMR pulse sequences and strategies have been proposed to circumvent these difficulties, (Bracken et al. 1997; Serber et al. 2001; Panchal et al. 2001; Bertini et al. 2003; Sun et al. 2005; Bermel et al. 2006, 2008; Bertini et al. 2008; Mukrasch et al. 2009; Frueh et al. 2009; Motackova et al. 2010; Mantylahti et al. 2010; Bagai et al. 2011; Mantylahti, Hellman and Permi 2011, Bermel et al. 2012, 2013a, b; Liu and Yang 2013; Isaksson et al. 2013). Non-linear sampling and analysis approaches (Schmieder et al. 1993; Hoch and Stern 2001; Korzhnev et al. 2001; Chen et al. 2003; Rovnyak et al.

Electronic supplementary material The online version of this article (doi:10.1007/s10858-014-9839-x) contains supplementary material, which is available to authorized users.

J. G. Reddy · R. V. Hosur (✉)
Department of Chemical Sciences, Tata Institute of Fundamental Research (TIFR), 1, Homi Bhabha Road, Colaba 400005, Mumbai, India
e-mail: hosur@tifr.res.in

R. V. Hosur
UM-DAE Centre for Excellence in Basic Sciences, University of Mumbai, Kalina Campus, Santa Cruz 400098, Mumbai, India

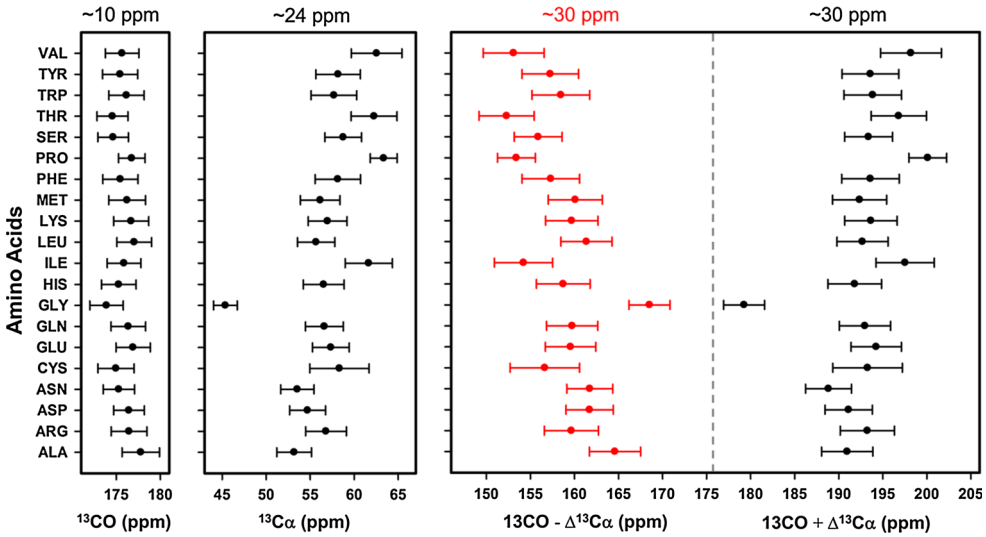

Fig. 1 Comparison between dispersion of individual ^{13}CO (*first panel*) and ^{13}Cα (*second panel*) chemical shifts and that of linear combination of these chemical shifts (*third panel*) for 20 common amino acids. In these plots the average chemical shifts are plotted against the residue types and standard deviations are shown as *error bars*. The average chemical shifts have been taken from the BMRB statistical table containing values calculated from the full BMRB database (Ulrich et al. 2008). In the last panel, linear combination of ^{13}CO and ^{13}Cα average chemical shifts for all the amino acid types calculated as reduced dimensionality convention (Szyperski et al. 1993, 2002) using 176 and 40 ppm as ^{13}CO and ^{13}Cα offset frequencies, respectively. The total chemical shift dispersion possibly achieved in each case has been shown at the top of each plot. Comparison clearly shows that the linear combination of ^{13}CO and ^{13}Cα chemical shifts can provide better dispersion compared to the individual chemical shifts

2004; Bruschweiler and Zhang 2004; Jaravine et al. 2006; Kazimierczuk et al. 2006; Billeter and Orekhov 2012) have been successfully employed to enhance the performance of these experiments. Even so, innovations continue and some of the key objectives of these efforts are: reducing the number of NMR experiments to obtain the required information, encoding maximum information in a single experiment, increasing the speed of data collection, and designing simple, easy to use, and efficient data analysis strategies.

In this context, we focus here on reduced dimensionality based experiments where information contained in a particular high dimensional experiment is extracted by performing a lower dimensional experiment (Szyperski et al. 1993, 2002). This is achieved by co-evolving more than one nucleus simultaneously along one or more particular time axes of the multidimensional experiment. It is easily conceivable that a variety of pulse sequences resulting in different spectral features can be generated by, (1) varying the nuclei that are to be frequency labeled, (2) varying the combinations of nuclei for co-evolution, (3) varying the magnetization transfer pathways along the backbone and (4) different optimizations of the data acquisition procedures. Indeed, a number of pulse sequences have already been published by such variations (Atreya et al. 2005; Chandra et al. 2012; Reddy and Hosur 2012; Rout et al. 2012; Szyperski et al. 2002). While working with disordered systems an additional point may be considered, and that is, ^{15}N and ^{13}CO chemical shift dispersions are much better than those of ^{1}HN and ^{13}CA chemical shifts in unfolded proteins (Dyson and Wright 2001; Bermel et al. 2013a). In this sense, N and CO combinations are expected to produce the best dispersions and, indeed, these experiments have been published (Löhr and Rüterjans 1995; Brutscher et al. 1995; Astrof et al. 2001; Kumar 2013b). Our motivation, presently, has been to extract maximum chemical shift information from a single experiment, without compromising too much on the spectral dispersion, and retaining the beneficial features such as 'check points' present in some of the previously described multi-dimensional experiments (Chatterjee et al. 2002; Kumar et al. 2010b). Thus, we decided to use in a 3D experiment, CO and CA combination along one of the axes, with the other two axes displaying ^{15}N and amide proton chemical shifts; it is worth mentioning that the chemical shift dispersion in (CO, CA) combination is better than that in individual CO and CA shifts (Fig. 1). This way, we will be able to extract four different backbone chemical shifts (^{1}HN, ^{15}N, ^{13}CO and ^{13}Cα) from a single experiment. We implemented this idea in the magnetization transfer pathway—$HN_i \rightarrow N_i \rightarrow CO_{i-1} \rightarrow CA_{i-1} \rightarrow N_{i,\ i-1} \rightarrow HN_{i,\ i-1}$ (Grzesiek et al. 1993)—as implemented in the HN(C)N experiment (Panchal et al. 2001; Chatterjee et al. 2002) so as to retain the beneficial 'check point' features of the latter from the point of view of sequential walk along the backbone. Although, in the present implementation we have not

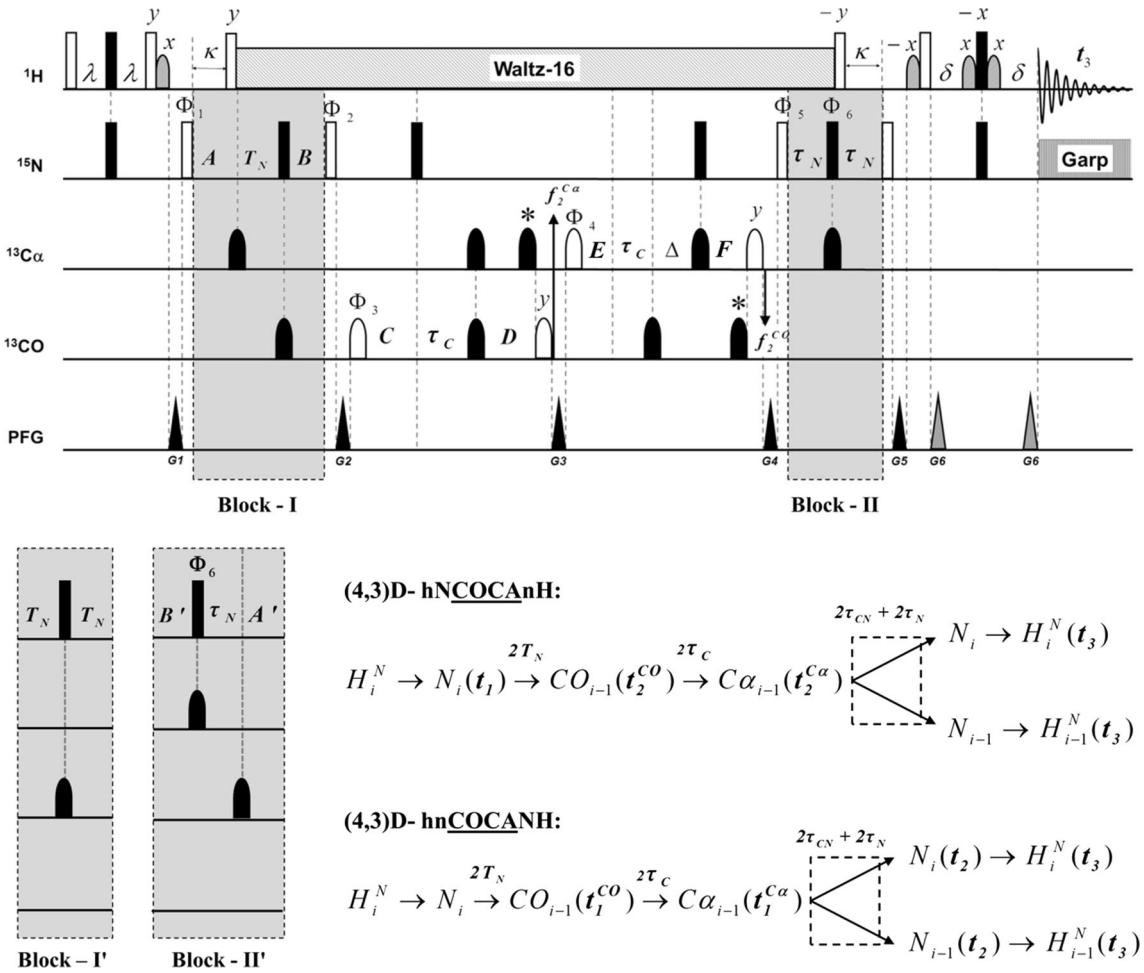

Fig. 2 Pulse sequence for (4,3)D-hNCOCAnH experiment. Hollow and *filled* (*black*) *rectangular bars* represent non-selective 90° and 180° pulses, respectively. Unless indicated, the pulses are applied with phase '*x*'. Proton decoupling using the waltz-16 decoupling sequence (Shaka et al. 1983) with field strength of 6.3 kHz is applied during most of the t_1 (^{15}N) and t_2 (^{13}C) evolution periods, and ^{15}N decoupling using the GARP-1 sequence (Shaka et al. 1985) with the field strength 0.9 kHz is applied during (t_3) acquisition. Standard Gaussian cascade pulses (Emsley and Bodenhausen 1990)—shape Q3 for 180° inversion (*filled black*; width 200 μs) and shape Q5 for 90° excitation (*hollow*, width 310 μs)—were used for band selective excitation and inversion along the ^{13}C channel. The strength of the ^{13}Cα pulses is adjusted so that they cause minimal excitation of carbonyl carbons and that of 180° ^{13}CO shaped pulse so that they cause minimal excitation of ^{13}Cα. Shaped pulses labeled with '*asterisk*' were applied for compensation of off-resonance effects (Bloch-Siegert phase shift) (Zhang and Gorenstein 2002). The values for the individual periods containing t_1 evolution of ^{15}N nuclei are: $A = t_1/2$ and $B = T_N - t_1/2$. The values for the time period containing 't_2^{CO}' evolution are: $C = t_2^{CO}/2$ and $D = \tau_C - t_2^{CO}/2$. The ^{13}Cα nuclei are co-evolved with for ^{13}CO nuclei in a constant time manner, and the values for the individual periods containing '$t_2^{C\alpha}$' evolution of ^{13}Cα nuclei are: $E = t_2^{C\alpha}/2$ and $F = \tau_{CN} - t_2^{C\alpha}/2$. Co-evolution ^{13}CO and ^{13}Cα nuclei are achieved by shifting the offset of the carbon channel (f_2) as shown by *vertical arrows*. The other delays are set to $\lambda = 2.5$ ms, $\kappa = 5.4$ ms, $\delta = 2.5$ ms, $T_N = 14$ ms, $\tau_C = 4.5$ ms, $\tau_{CN} = 12.5$ ms, $\tau_N = 13.5$ ms and $\Delta = \tau_{CN} - \tau_C$. The τ_{CN} must be optimized and is around 12–15 ms. The phase cycling for the experiment is $\Phi_1 = 2(x), 2(-x)$; $\Phi_2 = \Phi_3 = x, -x$; $\Phi_4 = \Phi_5 = x$; $\Phi_6 = 4(x), 4(-x)$; and Φ receiver $= 2(x), 4(-x), 2(x)$. The frequency discrimination in t_1 and t_2 has been achieved using States-TPPI phase cycling (Marion et al. 1989) of Φ_1 and Φ_3, respectively, along with the receiver phase. The gradient (*sine-bell shaped*; 1 ms) levels are as follows: G1 = 30 %, G2 = 30 %, G3 = 30 %, G4 = 30 %, G5 = 50 %, and G6 = 80 % of the maximum strength 53 G/cm in the z-direction. The recovery time after each gradient pulse was 160 μs. Before detection, WATERGATE sequence (Piotto et al. 1992) has been employed for better water suppression. Pulse scheme for (4,3)D-hnCOCANH experiment is same except block-I replaced by I' and block-II replaced by II' for chemical shift labeling of nitrogen in different position. The values for the individual periods containing t_2 evolution of ^{15}N nuclei in (4,3)D-hnCOCANH experiment are: $A' = t_2/2$ and $B' = \tau_N - t_2/2$. Pulse sequence code for both the experiments, (4,3)D-hNCOCAnH and (4,3)D-hnCOCANH, were included in supplementary materials. Schematic diagram of the magnetization transfer pathways and frequency labeling in (4,3)D-hNCOCAnH and (4,3)D-hnCOCANH pulse sequences are shown. $2T_N$, $2\tau_C$, $2\tau_{CN}$, and $2\tau_N$ are the delays during which the transfers indicated by the *arrows* take place in the pulse sequences

incorporated non-uniform sampling for the purpose of easy operation on all commercial spectrometers, it is needless to say that such incorporation would further enhance the performance of the experiment.

The above ideas generated two experiments (Fig. 2), one where the first nitrogen in the transfer pathway is frequency labeled, named as (4,3)D-hNCOCAnH, and the second where the second nitrogen at the end of the scheme before transferring magnetization back to amide protons for detection, is frequency labeled (replacing block—I with I′ and block—II with II′ in Fig. 2), which can be named as (4,3)D-hnCOCANH. Pulse sequence code for both the experiments, (4,3)D-hNCOCAnH and (4,3)D-hnCOCANH, have been included in supplementary materials. While the manuscript describing both of these was being prepared for submission we came across the publication of (4,3)D-hnCOCANH experiment by another group (Kumar 2013a). Therefore, we restrict our discussion here to the other experiment, namely, (4,3)D-hNCOCAnH and the sequential assignment using (4,3)D-hnCOCANH spectra recorded on unfolded human SUMO protein has been shown in supporting information (Figure S1). The (4,3)D-hNCOCAnH experiment presented here provides sequential (i − 1) ^{13}CO and ^{13}Cα chemical shift information along F_2 dimension, and self (i) and sequential (i − 1) amide ^{1}H chemical shift information in both F_1–F_3 and F_2–F_3 planes of the 3D spectrum. This is in a sense an advantage over the (4,3)D-hnCOCANH, since in that experiment the sequential information is present along the indirect dimension where the resolution is intrinsically limited compared to that along the direct dimension. Thus, in (4,3)D-hNCOCAnH even for a small difference in amide ^{1}H chemical shifts (even of the order of line width, ∼15 Hz) a sequential connectivity can be established. The experiment can also be recorded on deuterated samples, and the correlations in this experiment are resolved using three—^{15}N, ^{13}CO and ^{13}Cα—chemical shifts.

The reduced dimensionality experiments are in essence projection experiments. It is worthwhile, therefore to compare the present experiment with some of such experiments which give similar information. Very recently a pair of experiments, (4,3)D hNCOcaNH and (4,3)D hNcoCANH, were developed which relied upon the N(i) ± CO(i − 1) and N(i) ± CA(i − 1) chemical shift dispersions, respectively (Kumar 2013b). These also yield good dispersion, but, clearly, two experiments are required for obtaining both Cα and CO chemical shifts. Whereas in the experiment presented here, we get $HN_{i,i-1}$, N_i, $C\alpha_{i-1}$ and CO_{i-1} assignments from a single 3D experiment. In 6D APSY HNCOCANH experiment presented by Fiorito et al. (Fiorito et al. 2006), several 2D projections of the 6D experiment are recorded and these are automatically analysed with the software GAPRO (Hiller et al. 2005) to generate a precise 6D peak list. This peak list is then automatically analysed using the software GARANT (Bartels et al. 1997) to obtain sequence specific assignments of the backbone atoms. The authors also tuned the experiment for suppressing magnetization transfer through $^{2}J_{NCA}$ coupling, so as to reduce the number of peaks (self peaks are suppressed) on one hand and enhance the transfer efficiency to the sequential peaks on the other. In this scenario, the suppression of self-peaks becomes necessary, since the self and sequential peaks have opposite signs and while taking 2D projections of the 6D spectrum, there can be severe cancellations leading to loss of information. This is achieved by selecting a 50 ms transfer delay. This has been demonstrated to work very well in small proteins (Fiorito et al. 2006). However, a particular shortcoming here is that during the long transfer delay used, the coherence resides on Cα, and since relaxation of Cα is very efficient (especially, in the absence of deuteration), this causes substantial loss of sensitivity. In contrast, in (4,3)D hNCOCAnH experiment the transfer time is only 25 ms. So, the relaxation losses are less, both self and sequential information are obtained (as both ^{1}J and ^{2}J-NCA transfers are selected) along the high resolution (direct detection) dimension, and this is an advantage since special peak patterns of positive and negative signs arise for self and sequential peaks for particular residue types (see later) which serve as check/start points during sequential assignment walk along the backbone. Although the self and sequential peaks have opposite signs there are no severe cancellation problems in the 3D spectrum as two sets of such peaks with different combinations of chemical shifts appear in the reduced dimensionality spectra. Thus these advantages of spectral features and lower relaxation losses more than compensate for the slightly higher transfer efficiency for the sequential peaks in the 6D-APSY spectrum. The performance of the (4,3)D-hNCOCAnH experiment and the application of the method have been demonstrated using intrinsically disordered α-synuclein protein. We also describe a protocol, wherein this experiment when combined with HNN (Panchal et al. 2001; Kumar et al. 2010a) allows removal of some ambiguities arising due to degeneracy of amide proton chemical shifts, and identification of sequentially connected peaks in the HSQC spectrum can be accomplished.

Materials and methods

The proposed reduced dimensionality experiment-(4,3)D-hNCOCAnH (Fig. 2) was developed and successfully first optimized using a uniformly ^{15}N/^{13}C labeled human ubiquitin (76 amino acids, final concentration ∼1.0 mM) dissolved in acetate buffer pH 5.0 in 90 % H_2O and 10 %

D_2O. Application of the experiment on unfolded or intrinsically disordered proteins has been demonstrated using 14.4 kDa intrinsically disordered α-synuclein (140 amino acids) protein. The $^{13}C/^{15}N$ labeled NMR sample of α-synuclein protein (~0.8 mM) in phosphate buffer containing 90 % H_2O and 10 % D_2O and pH 6.0 has been prepared as described elsewhere (Ghosh et al. 2013). Experiments on α-synuclein were performed at 288 K. All the experiments were recorded on Bruker Avance III NMR spectrometer operating at ^1H frequency of 800 MHz and equipped with a cryoprobe. Acquisition parameters of the spectra recorded are shown in Table 1. The ^{13}C carrier frequencies for pulses in $^{13}C\alpha$ and ^{13}CO channels in all experiments were set at 54.0 ppm and 173.0 ppm, respectively. Data was processed using Topspin (BRUKER, http://www.bruker.com/) software and analyzed using CARA software (Keller 2004).

Results and discussion

Pulse sequence and magnetization transfer

The pulse sequence for (4,3)D-hNCOCAnH experiment for establishing correlations between sequential HSQC peaks (i.e. from $H_iN_i \rightarrow H_{i-1}N_i \rightarrow H_{i-1}N_{i-1}$) is shown in Fig. 2. It has been derived from the previously described HN(C)N pulse sequence (Panchal et al. 2001; Bracken et al. 1997) and differs in the way the t_2 evolution is handled. The magnetization transfer pathway and the frequency labeling steps in (4,3)D-hNCOCAnH pulse sequence are explicitly depicted in Fig. 2; the t_2 evolution involves joint sampling of backbone ^{13}CO and $^{13}C\alpha$ chemical shifts of preceding residue $(i-1)$. The theoretical description of the pulse sequence goes identical to that of HN(C)N, except that the frequencies along the t_2 indirect dimension will be sums and differences of frequencies of the jointly sampled nuclei. Here, $^{13}CO_{i-1}$ chemical shifts are detected in quadrature whereas alpha carbon ($^{13}C\alpha_{\ i-1}$) chemical shifts modulate the transfer amplitude. Overall, the experiment-encoding 4D spectral information-results in a simple three dimensional (3D) spectrum which preserves all the beneficial features of HN(C)N spectrum, especially the positive and negative peak patterns (Chatterjee et al. 2002).

Table 1 Acquisition parameters of the experiments recorded on intrinsically disordered α-synuclein protein

Protein sample	Intrinsically disordered α-synuclein protein	
Experiment	(4,3)D-hNCOCAnH	3D-HNN
Spectral width (offset) in ppm ($^{13}CO/^{13}C\alpha$)*	$F_3(^1H) = 9.0$ (4.7) $F_2(^{13}C^{+/-}) = 50.0$ (173.0/40.0)* $F_1(^{15}N) = 26.0$ (119.0)	$F_3(^1H) = 9.0$ (4.7) $F_2(^{15}N) = 26.0$ (119.0) $F_1(^{15}N) = 26.0$ (119.0)
Complex data points $F_3 \times F_2 \times F_1$	1,024 × 128 × 48	1,024 × 56 × 56
Scans per FID (inter scan delay)	16 (0.8 s)	16 (0.8 s)
Experiment time	~30 h	~15 h 30 min

The salient features of the (4,3)D-hNCOCAnH spectrum are briefly described in the following paragraphs. As shown schematically in Fig. 3a, the peaks appear at the following coordinates in the spectrum:

$$F_1 = N_i, (F_2, F_3) = \left(C^+_{i-1}, H_i\right), \left(C^+_{i-1}, H_{i-1}\right), \left(C^-_{i-1}, H_i\right), \left(C^-_{i-1}, H_{i-1}\right)$$

$$F_2 = C^+_{i-1}/C^-_{i-1}, (F_1, F_3) = (N_i, H_i), (N_i, H_{i-1})$$

The letters "H" and "N" here refer to amide ^1H and ^{15}N chemical shifts, whereas the letters "C^+_{i-1}" and "C^-_{i-1}" refer to the linear combination of $^{13}CO_{i-1}$ and $^{13}C\alpha_{i-1}$ chemical shifts (where i is residue number). Depending upon the offset used along ^{13}C channel during the $^{13}C\alpha$ chemical shift evolution (i.e. $^{13}C\alpha_{\ offset}$), the values of linearly combined chemical shifts are evaluated according to reduced dimensionality NMR convention: (Szyperski et al. 2002, 1993)

$$C^+_{i-1} = CO_{obs} + (C\alpha_{obs} - C\alpha_{offset})$$

$$C^-_{i-1} = CO_{obs} - (C\alpha_{obs} - C\alpha_{offset})$$

Peak patterns

Schematic (4,3)D-hNCOCAnH spectrum and the correlations observed in the $F_1(^{15}N)$–$F_3(^1H)$ and $F_2(^{13}C^{+/-})$–$F_3(^1H)$ planes are shown in Fig. 3a. The F_2–F_3 plane at $F_1 = N_i$, shows four correlation peaks in which two are up-field and two are down-field from the offset ($^{13}CO_{offset}$), due to the addition and subtraction of $^{13}C\alpha$ frequencies (Fig. 3a, left panel), respectively. One peak from each set (up-fielded/down-fielded) is an intra-residue correlation peak, (C^+_{i-1}, H_{i-1} and C^-_{i-1}, H_{i-1}) and the other is an inter-residue correlation peak, (C^+_i, H_{i-1} and C^-_i, H_{i-1}). The F_1–F_3 plane corresponding to $F_2 = {}^{13}C^+_{i-1}/{}^{13}C^-_{i-1}$, shows an intra-residue peak (N_i, H_i) and an inter-residue (N_i, H_{i-1}) correlation peak referred here as self and sequential peaks, respectively, (Fig. 3a, right panel). Like in HN(C)N experiment, the inter- and intra-residue correlation peaks in different planes of (4,3)D-hNCOCAnH spectrum have opposite signs except for some special cases. Considering different triplets of residues, covering general and all

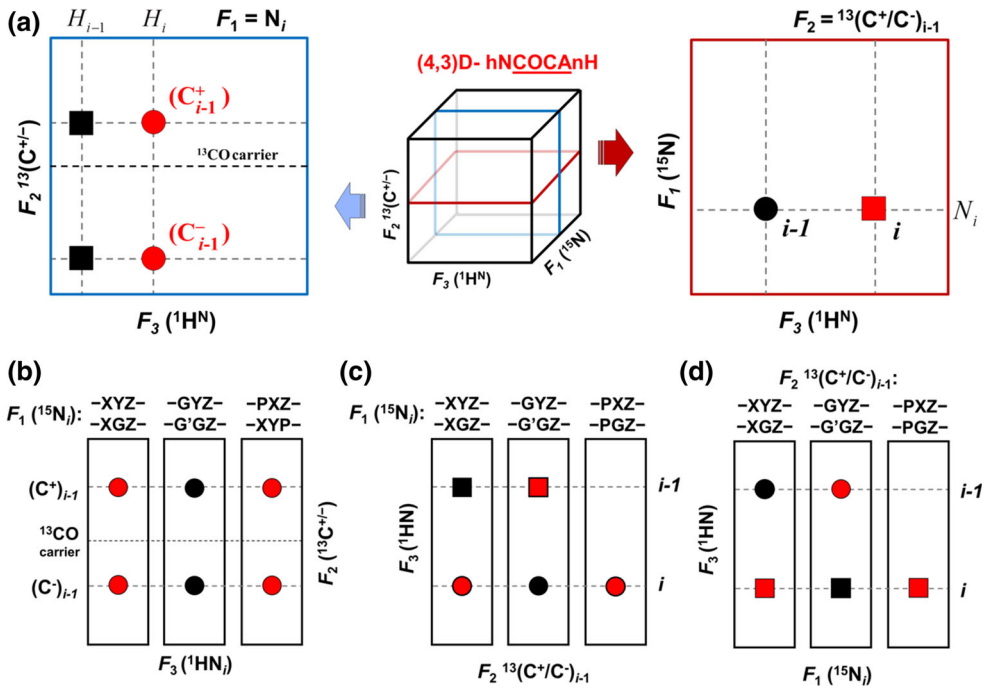

Fig. 3 **a** Schematic three-dimensional spectrum of (4,3)D-hNCOCAnH experiment and the correlations observed in the F_1–F_3 (*right side*) and F_2–F_3 (*left side*) planes, respectively, at the ^{15}N chemical shifts of residue i and $^{13}C^+/^{13}C^-$ chemical shifts of residue $i-1$. *Squares* and *circles* represent the self and sequential peaks, respectively. *Red* and *black* represent positive and negative phase of peaks, respectively. **b** Schematic peak patterns in the $F_2(^{13}C^{+/-})$–$F_3(^1H)$ planes of the (4,3)D-hNCOCAnH spectrum at the $^{15}N_i$ chemical shift of the central residue (i) in the triplet mentioned on the top of each panel. Schematic peak patterns in **c** $F_2(^{13}C^{+/-})$–$F_3(^1H)$ and **d** $F_1(^{15}N)$–$F_3(^1H)$ planes of the (4,3)D-hNCOCAnH spectrum, respectively, at the $^{15}N^i$ and $^{13}C^+_{i-1}/^{13}C^-_{i-1}$ chemical shifts corresponding to the central residue (i) in the triplet mentioned on the top of each panel. X, Y and Z are any residues other than glycine and proline. G/G′ and P represent glycine and proline, respectively. Special patterns of self and sequential peaks appear when there is G or P at $i-1$ position in the triplet sequence and thus provide identification of spin-systems following glycines and prolines in the sequence which help during the sequential assignment walk along the sequence

special situations, the expected peak patterns in the F_1–F_3 and F_2–F_3 planes of the (4,3)D-hNCOCAnH spectrum are shown schematically in Fig. 3, where intra- and inter-residue correlation peaks have been shown as squares and circles, respectively. Different patterns arise for different triplet stretches of residues. Figure 3b, c shows the expected peak patterns (for the triplet stretches shown above each panel) in the $F_2(^{13}C^{+/-})$–$F_3(^1H)$ planes of the spectrum at the F_1 ($^{15}N_i$) chemical shift of the central residue, i. Each panel in Fig. 3b represents the strip of the plane centered about the amide ^1H_i chemical shift of the central residue, i, of the triplet and each panel in Fig. 3c represents the strip centered about the $^{13}C^+_{i-1}/^{13}C^-_{i-1}$ chemical shift of the first residue of the triplet (i.e. $i-1$). Figure 3d shows the expected peak patterns (for the triplet stretches shown above each panel) in the $F_1(^{15}N)$–$F_3(^1H)$ planes of the spectrum at the $F_2(^{13}C^+_{i-1}/^{13}C^-_{i-1})$ chemical shift of residue, $i-1$. Each panel shows the strip of the plane centered about the $^{15}N_i$ chemical shift of the central residue, i, of the triplet. The red and black squares/circles represent positive and negative peaks, respectively. The actual signs in the spectrum are dictated by whether the $i-1$ residue is a glycine or otherwise, and of course by the phasing of the spectra. Here, we have made the intra-residue correlation peak positive and inter-residue correlation peak negative for a triplet sequence –XYZ–, where X, Y and Z are any residues other than glycines and prolines which have been represented by letters 'G' and 'P', respectively. For glycines, the evolution of the magnetization components is slightly different because of the absence of the β-carbon. This, in turn, generates some special patterns depending on whether the $(i-1)$th residue is a glycine or otherwise, see middle panels of Fig. 3b–d. Note that prolines which do not have amide proton give rise to further special patterns in the spectrum. Prolines, at position $i-1$ in the triplet stretches, results in (a) absence of the intra-residue correlation peak (H_{i-1}, C^+_{i-1} and H_{i-1}, C^-_{i-1}) in $F_2(^{13}C^{+/-})$–$F_3(^1H)$ plane of the spectrum at the F_1 ($^{15}N_i$) chemical shift of residue, i (see last panel in Fig. 3c) and (b) absence of the inter-residue correlation peak (H_i, N_{i-1}) in $F_1(^{15}N)$–$F_3(^1H)$ plane of the hNCOCAnH spectrum at the F_2 ($^{13}C^+/^{13}C^-$) chemical

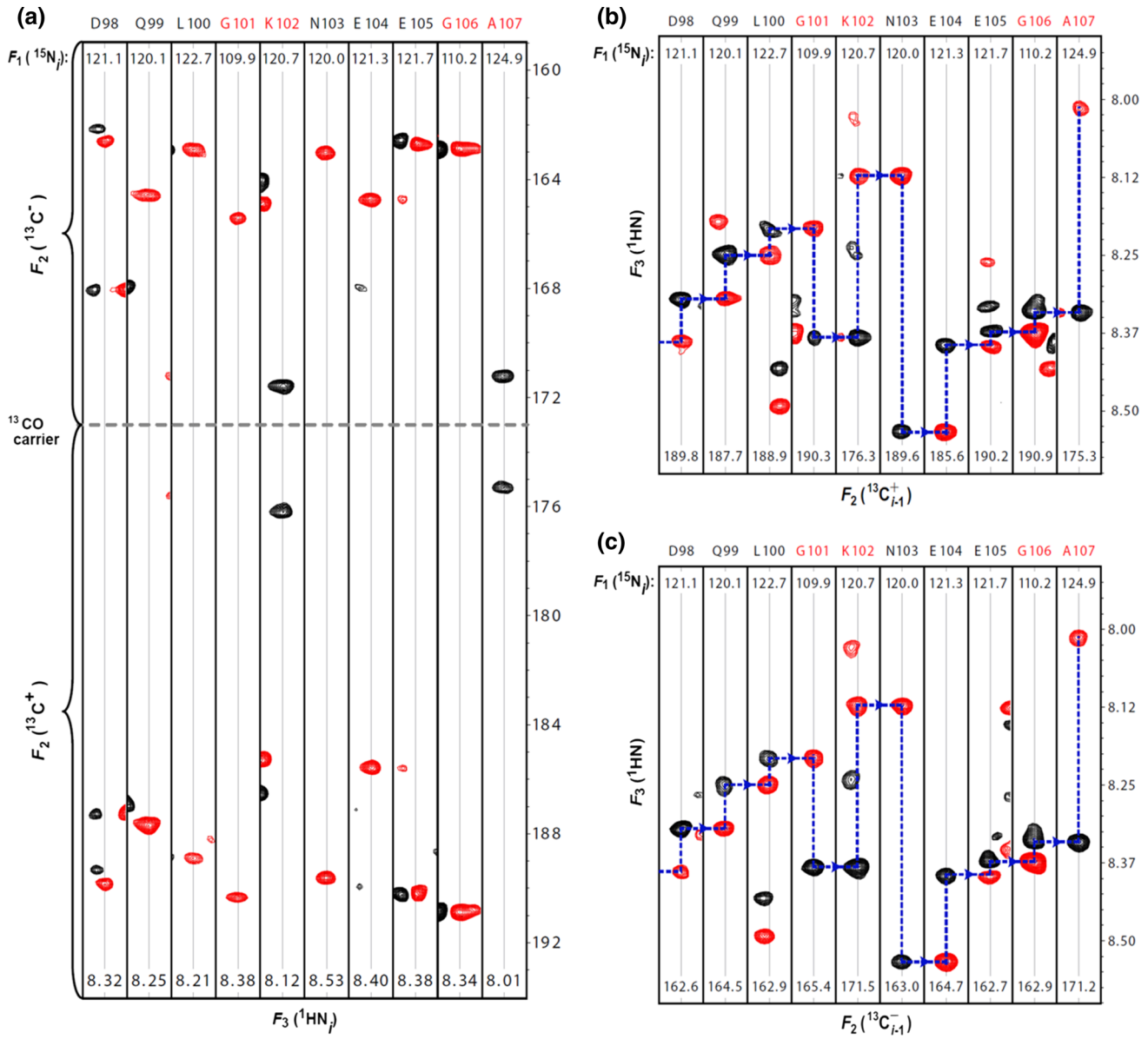

Fig. 4 Sequential resonance assignment of a continuous stretch from D98-A107 using different planes of (4,3D)-hNCOCAnH spectrum recorded on α-synuclein protein. **a** The strips are taken from the $F_2(^{13}C^{+/-})$–$F_3(^{1}H)$ planes at $F_1(^{15}N_i)$ chemical shift and are centered about the corresponding amide chemical shift (i.e. $^{1}H_i$) of residue mentioned above the panels. The strips are showing (H_i, C^{+}_{i-1}) (down-fielded) and (H_i, C^{-}_{i-1}) (up-fielded) correlation peaks which are linear combination of sequential $(i-1)$ ^{13}CO and ^{13}Cα chemical shifts. **b** $F_2(^{13}C^{+})$–$F_3(^{1}H)$ planes and **c** $F_2(^{13}C^{-})$–$F_3(^{1}H)$ taken at $F_1(^{15}N)$ chemical shift of residues mentioned above the panel and are centered about the corresponding $^{13}C^{+}_{i-1}$ and $^{13}C^{-}_{i-1}$ chemical shifts, respectively of the residue mentioned above the panels.*Red and black contours* indicate positive and negative peaks. *Horizontal lines* in (**b**) and (**c**) connect a self $(^{1}H_i)$ correlation peak in one plane to a sequential $(^{1}H_{i-1})$ correlation peak in the adjacent plane on the right. Note that the peaks in K102 and A107 planes following G101 and G106 respectively, in the sequence appear with different phase and thus provide an internal check while transforming the stretches of sequentially connected peaks into the final assignment

shift of residue, $i-1$ (see last panel in Fig. 3d). These special peak patterns—which help in the identification of the residues following glycines and prolines in the sequence-provide important start/check points and stop/break points during the course of the sequential assignment process.

Assignment protocol

Keeping in mind the distinctive features of the (4,3)D-hNCOCAnH spectrum, we describe below the assignment protocol using this spectrum, and α-synuclein, a protein that has been extensively studied in the literature (Kang

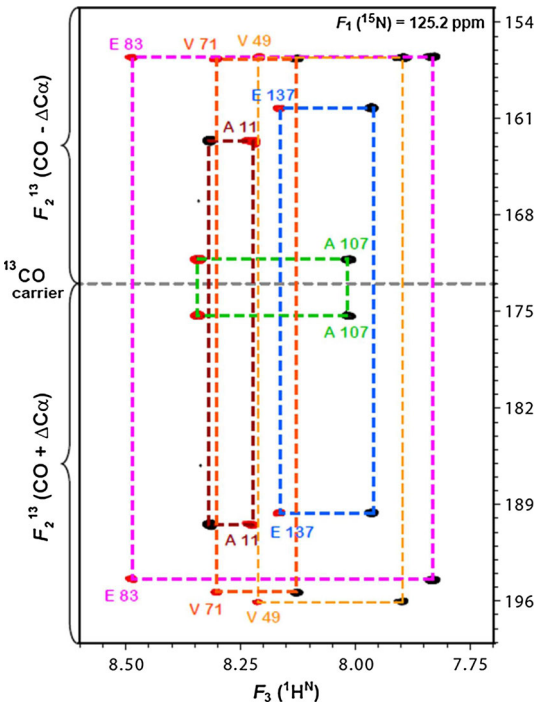

Fig. 5 An illustrative example showing unambiguous identification of self (i) and sequential ($i-1$) amide ^{1}H chemical shifts of A11, V49, V71, E83, A107 and E137 residues using $F_2(^{13}C^{+/-})$–$F_3(^{1}H)$ plane of (4,3)D-hNCOCAnH spectrum taken at degenerate ^{15}N chemical shift (125.2 ppm). The *red* and *black* contours indicate positive and negative peaks, respectively

et al. 2013; Rao et al. 2009; Bermel et al. 2013a, 2006) has been used as the model IDP system. The assignment protocol relies on (1) sequential amide ^{1}H/^{15}N and ^{13}CO $\pm$ Δ^{13}Cα correlations and (2) the distinctive peak patterns of intra- and inter-residue correlation peaks in different planes of the (4,3)D-hNCOCAnH spectrum which enable ready identification of certain specific triplet stretches especially containing glycines and prolines (Fig. 3). First, the backbone amide spin-systems are identified in the ^{15}N $-$ ^{1}H HSQC spectrum. For each spin-system i, the $^{13}C^{+}_{i-1}$ and $^{13}C^{-}_{i-1}$ chemical shift are identified from the $F_2(^{13}C^{+/-})$–$F_3(^{1}H)$ plane of the (4,3)D-hNCOCAnH spectrum at the $F_1(^{15}N_i)$ chemical shift (Fig. 4a). The same plane also provides unambiguous identification of $^{1}H_{i-1}$ chemical shift on the strip along $F_3(^{1}H)$ dimension centered about the $^{13}C^{+}_{i-1}$ and $^{13}C^{-}_{i-1}$ chemical shifts (Fig. 4b, c). For a spin-system, the sequential $^{1}H_{i-1}$ chemical shift can also be identified from $F_1(^{15}N)$–$F_3(^{1}H)$ plane of the (4,3)D-hNCOCAnH spectrum at $F_2(^{13}C^{+}_{i-1}/^{13}C^{-}_{i-1})$ chemical shift. This identification is made on the strip along $F_3(^{1}H)$ dimension centered about the $^{15}N_i$ chemical shift (Figure S2). Further, if there is ambiguity in the identification of $^{1}H_{i-1}$ chemical shift in $F_1(^{15}N)$–$F_3(^{1}H)$ plane due to ^{15}N chemical shift degeneracy, it can be resolved using the $F_2(^{13}C^{+/-})$–$F_3(^{1}H)$ plane (Fig. 5). Further, if the amide ^{1}H chemical shifts are unique, the identified sequential $^{1}H_{i-1}$chemical shift can be used to establish the sequential connectivities between the HSQC peaks from the (4,3)D-hNCOCAnH spectrum. This is indeed true for small well-folded proteins and one can get complete assignment based on the sequential amide correlations in combination with glycines, alanine, and serine/threonine check points identified during sequential walk. Illustrative stretches of sequential walk through different planes of (4,3)D-hNCOCAnH spectrum recorded on intrinsically disordered (140 aa) α-synuclein protein are shown in Figure S2 and Fig. 4. In Figures S2A and S2B, the intra-residue correlation peak (H_i, N_i in red) in one plane joins the inter-residue correlation peak (H_{i-1}, N_i in black) in the adjacent plane on the right. In Fig. 4b, c, the inter-residue correlation peak ($H_i, C^{+}_{i-1}/C^{-}_{i-1}$ in red) in one plane joins the intra-residue correlation peak ($H_{i-1}, C^{+}_{i-1}/C^{-}_{i-1}$ in black) in the adjacent plane on the right. Note that G101, G106, K102 and A107 panels constitute the check points in this sequential walk.

The stretches of sequentially connected spin-systems are transformed into a primary sequence format highlighting the residues identified in the sequential walk, like—BGXBXBXXXXP—where (1) P stands for proline (indicated by missing intra-residue H_{i-1},C^{+}_{i-1} and H_{i-1},C^{-}_{i-1} correlation peaks), (2) G, A and B represent spin-systems identified as glycines, alanines and serines/threonines, respectively, and (3) X represents a spin-system other than proline, glycine, alanine and serine/threonine. Now the transformed stretches of sequentially connected spin-systems are compared with the primary sequence to find a match. In presence of sufficient number of check points that are generally available for glycines, alanines, serines/threonines and prolines; explicit side chain assignment would not be very necessary to decide the correctness of the sequential assignment. Moreover, these intra- and inter-residue correlations to amide protons are seen in the direct dimension, which has maximum resolution compared to the indirect (^{15}N and ^{13}C) dimensions. Thus, even a small difference (perhaps as low as the line width itself) in amide ^{1}H chemical shift can be resolved.

Nonetheless, ambiguities may arise in case of total degeneracies along amide ^{1}H chemical shifts. For such situations, we use additional information from 3D-HNN spectrum (Kumar et al. 2010a; Panchal et al. 2001). This combined assignment strategy is demonstrated in Fig. 6 for the stretch V66-G67-G68-A69 of α-synuclein, where the amide chemical shifts of V66 and G68 are highly degenerate. The sequential walk starts from a HSQC peak identified for a residue next to a glycine (residue A69 in

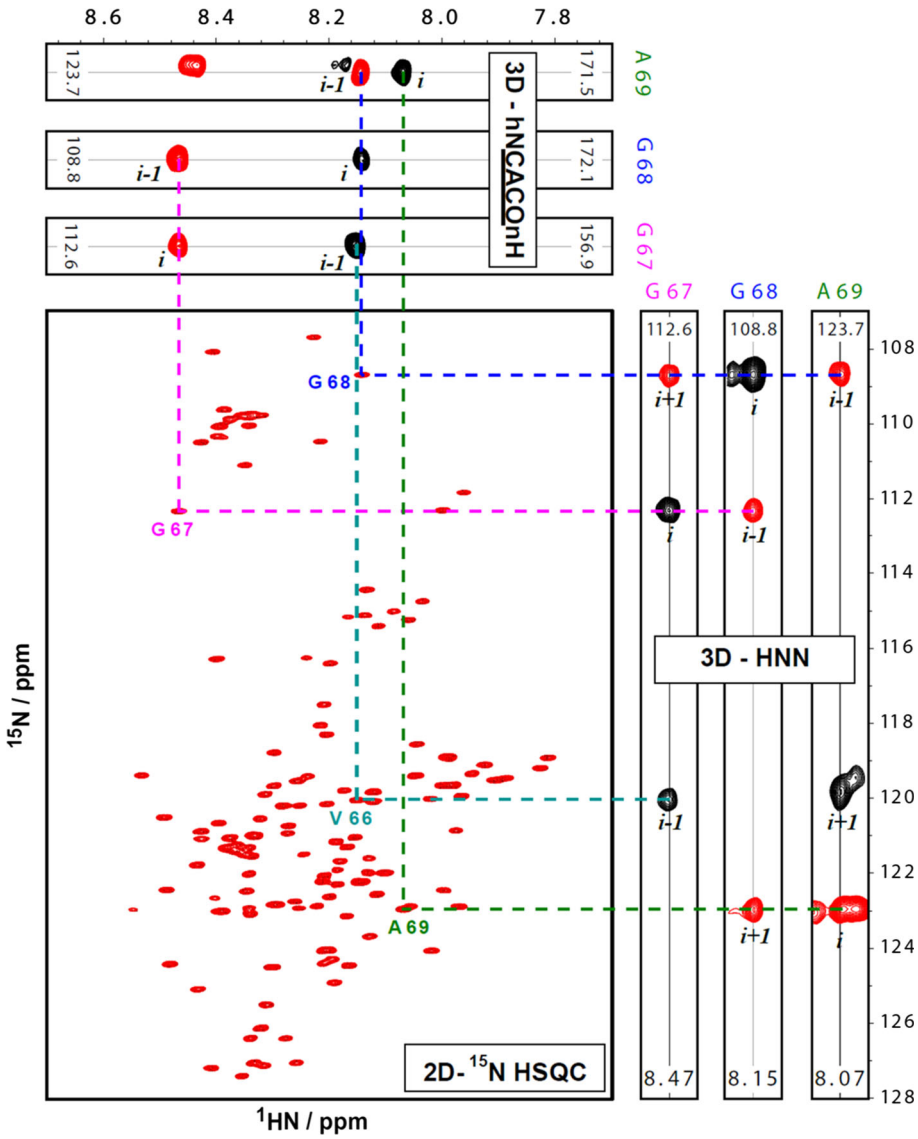

Fig. 6 Sequential resonance assignment of a continuous stretch from A69-G68-G67-V66, covering special situation like double glycine stretch, using (4,3D)-hNCOCAnH and 3D-HNN spectra recorded on α-synuclein. *Horizontal panels* are $F_1(^{15}N)$–$F_3(^{1}H)$ planes of (4,3)D-hNCOCAnH spectrum taken at $F_2(^{13}C^{+}_{i-1})$ chemical shift of residues mentioned above the panel and are centered about the corresponding $^{15}N_i$ chemical shift. *Vertical panels* are $F_1(^{15}N)$–$F_3(^{1}H)$ planes of 3D-HNN spectrum taken at $F_2(^{15}N_i)$ chemical shift of residues mentioned above the panel and are centered about the corresponding amide $^{1}H_i$ chemical shift. *Red* and *black* contours indicate positive and negative peaks

Fig. 6), which shows reverse peak patterns in the (4,3)D-hNCOCAnH spectrum (see middle panel in Fig. 3c, d). The sequential $(i-1)$ $^{13}C^{+}/^{13}C^{-}$ and sequential $(i-1)$ amide ^{1}H chemical shifts are identified unambiguously from (4,3)D-hNCOCAnH spectrum (as described above and Fig. 4). In the HNN spectrum the self peak of A69, along F_1 dimension is identified directly from the (H_i, N_i) correlation peak in the ^{15}N-HSQC spectrum. The HNN peak pattern for residue next to glycine (A69) is specific in providing unambiguous identification of sequential $i-1$ and $i+1$ amide ^{15}N chemical shifts which are discriminated, respectively, by their negative and positive peak signs (Fig. 6). The sequential $(i-1)$ amide ^{1}H chemical shift information obtained from (4,3)D-hNCOCAnH spectrum is then combined with the sequential $(i-1)$ amide ^{15}N chemical shift information derived from HNN spectrum to identify the sequential (H_{i-1}, N_{i-1}) HSQC peak (i.e. G68). Moving further with this information, the sequential (G67) amide ^{1}H chemical shift for HSQC peak G68 is identified from the (4,3)D-hNCOCAnH spectrum and sequential (G67) amide ^{15}N chemical shift is confirmed from the HNN spectrum. Thus, the sequential connectivities between the HSQC peaks (i.e. A69 → G68 → G67) can be established in a very simple and straightforward manner.

^{1}HN, ^{15}N, ^{13}CO and ^{13}Cα chemical shifts from (4,3)D-hNCOCAnH spectrum

The above assignment protocol resulted in complete assignment of the peaks in the spectrum. From these, the backbone ^{13}CO and ^{13}Cα chemical shifts were calculated using the $^{13}C^{+}_{i-1}$ and $^{13}C^{-}_{i-1}$ chemical shifts as follows:

$$^{13}CO_{i-1}^{obs} = (C_{i-1}^{+} + C_{i-1}^{-})/2$$

$$^{13}C\alpha_{i-1}^{obs} = C\alpha_{offset} + [(C_{i-1}^{+} - C_{i-1}^{-})/2]$$

Figure S3 documents the ^{15}N-HSQC peak annotations for α-synuclein protein and Table S1 documents all the chemical shifts obtained here. At this stage it may be worthwhile mentioning about the previous approaches to obtain the same assignments. In several of the studies, resonance assignment of α-synuclein has been characterized using conventional HNCO, HNC(CA)CO, CBCA(CO)NH and CBCANH experiments (Kang et al. 2013; Rao et al. 2009; Wu and Baum 2011). Each one of these experiments was run for a day or more. Recently, an extensive set of experiments based on ^{13}C direct detection has been proposed specially for the characterization of IDPs, where several 4D and 5D experiments along with non-uniform sampling approach were used for obtaining the assignments of α-synuclein protein (Bermel et al. 2012, 2013a, 2006). In all these cases the self and the sequential peaks have same phase and hence are often difficult to distinguish. This necessitates the use of two experiments in combination. In the present case, (4,3)D-hNCOCAnH alone led to assignment of 118 peaks in the ^{15}N HSQC spectrum and when used in conjunction with 3D-HNN, all the 133 peaks could be assigned. Along with that carbon assignments were also obtained. The overall experimental time in our approaches was significantly lower than that in the previous cases.

Conclusions

In conclusion, an efficient reduced dimensionality based method for high-throughput assignment of backbone (^{1}HN, ^{15}N, ^{13}CO, and ^{13}Cα) resonances of proteins has been presented. The (4,3)D-hNCOCAnH experiment exploits the ^{15}N, ^{13}CO and ^{13}Cα chemical shift dispersion which helps in unambiguous identification of self and sequential correlations. Moreover, it provides unidirectional $i \rightarrow i-1$ amide ^{1}H correlations along highly resolved (detection) dimension. Following the sequence specific patterns, (4,3)D-hNCOCAnH experiment alone can in principle provide complete sequence specific assignment. Further, (4,3)D-hNCOCAnH experiment together with 3D-HNN can provide a substantial boost to the sequential assignment process. This assignment protocol based on (4,3)D-hNCOCAnH and 3D-HNN spectra is quite simple and straight forward and one can directly identify the sequentially connected HSQC peak unambiguously after the manual peak picking process. We have demonstrated here the utility of the method for the generally more challenging intrinsically disordered proteins using α-synuclein as a model system. Indeed, the protocol can also be used for studying folded proteins. Thus, the experiments and the protocols described here will be great tool for backbone resonance assignment in structural and functional proteomics, protein folding, and drug discovery research programs by NMR, and are particularly invaluable in the case of IDPs.

Acknowledgments We thank Government of India for providing financial support to the National Facility for High Field NMR at Tata Institute of Fundamental Research, India. We would like to acknowledge Dr. Ashutosh Kumar and Priyatosh Ranjan (Biosciences and Bioengineering Department, IITB, Mumbai) for providing ^{13}C/^{15}N-labeled α-synuclein.

References

Astrof NS, Lyon CE, Griffin RG (2001) Triple Resonance Solid State NMR Experiments with Reduced Dimensionality Evolution Periods. J Magn Reson 152:303–307

Atreya HS, Eletsky A, Szyperski T (2005) Resonance assignment of proteins with high shift degeneracy based on 5D spectral information encoded in G2FT NMR experiments. J Am Chem Soc 127:4554–4555

Bagai I, Ragsdale SW, Zuiderweg ERP (2011) Pseudo-4D triple resonance experiments to resolve HN overlap in the backbone assignment of unfolded proteins. J Biomol NMR 49:69–74

Bartels C, Güntert P, Billeter M, Wüthrich K (1997) GARANT-a general algorithm for resonance assignment of multidimensional nuclear magnetic resonance spectra. J Comput Chem 18:139–149

Bermel W, Bertini I, Felli IC, Lee Y-M, Luchinat C, Pierattelli R (2006) Protonless NMR Experiments for Sequence-Specific Assignment of Backbone Nuclei in Unfolded Proteins. J Am Chem Soc 128:3918–3919

Bermel W, Felli IC, Kümmerle R, Pierattelli R (2008) 13C Direct-detection biomolecular NMR. Concepts Magn Reson Part A 32:183–200

Bermel W, Bertini I, Felli I, Gonnelli L, Koźmiński W, Piai A, Pierattelli R, Stanek J (2012) Speeding up sequence specific assignment of IDPs. J Biomol NMR 53:293–301

Bermel W, Bruix M, Felli I, Kumar MV, Pierattelli R, Serrano S (2013a) Improving the chemical shift dispersion of multidimensional NMR spectra of intrinsically disordered proteins. J Biomol NMR 55:231–237

Bermel W, Felli I, Gonnelli L, Koźmiński W, Piai A, Pierattelli R, Zawadzka-Kazimierczuk A (2013b) High-dimensionality 13C direct-detected NMR experiments for the automatic assignment of intrinsically disordered proteins. J Biomol NMR 57:353–361

Bertini I, Felli IC, Kümmerle R, Moskau D, Pierattelli R (2003) 13C–13C NOESY: an attractive alternative for studying large macromolecules. J Am Chem Soc 126:464–465

Bertini I, Jiménez B, Pierattelli R, Wedd AG, Xiao Z (2008) Protonless 13C direct detection NMR: characterization of the 37 kDa trimeric protein CutA1. Proteins Struct Funct Bioinf 70:1196–1205

Billeter M, Orekhov V (2012) Novel sampling approaches in higher dimensional NMR. Springer, New York

Bracken C, Palmer AG 3rd, Cavanagh J (1997) (H)N(COCA)NH and HN(COCA)NH experiments for 1H–15 N backbone assignments in 13C/15 N-labeled proteins. J Biomol NMR 9:94–100

Bruschweiler R, Zhang F (2004) Covariance nuclear magnetic resonance spectroscopy. J Chem Phys 120:5253–5260

Brutscher B, Cordier F, Simorre J-P, Caffrey M, Marion D (1995) High-resolution 3D HNCOCA experiment applied to a 28 kDa paramagnetic protein. J Biomol NMR 5:202–206

Chandra K, Jaipuria G, Shet D, Atreya HS (2012) Efficient sequential assignments in proteins with reduced dimensionality 3D HN(CA)NH. J Biomol NMR 52:115–126

Chatterjee A, Bhavesh NS, Panchal SC, Hosur RV (2002) A novel protocol based on HN(C)N for rapid resonance assignment in (N-15, C-13) labeled proteins: implications to structural genomics. Biochem Biophys Res Commun 293:427–432

Chen JH, De Angelis AA, Mandelshtam VA, Shaka AJ (2003) Progress on the two-dimensional filter diagonalization method. An efficient doubling scheme for two-dimensional constant-time NMR. J Magn Reson 162:74–89

Dyson HJ, Wright PE (2001) Nuclear magnetic resonance methods for elucidation of structure and dynamics in disordered states. NMR Biol Macromol Pt B 339:258–270

Dyson HJ, Wright PE (2004) Unfolded proteins and protein folding studied by NMR. Chem Rev 104:3607–3622

Eliezer D (2006) Characterizing residual structure in disordered protein states using nuclear magnetic resonance. In: Bai Y, Nussinov R (eds) Protein folding protocols. Humana Press, New York, pp 49–67

Emsley L, Bodenhausen G (1990) Gaussian pulse cascades: new analytical functions for rectangular selective inversion and in-phase excitation in NMR. Chem Phys Lett 165:469–476

Felli IC, Pierattelli R (2012) Recent progress in NMR spectroscopy: toward the study of intrinsically disordered proteins of increasing size and complexity. IUBMB Life 64:473–481

Fiorito F, Hiller S, Wider G, Wüthrich K (2006) Automated resonance assignment of proteins: 6D APSY-NMR. J Biomol NMR 35:27–37

Frueh DP, Arthanari H, Koglin A, Walsh CT, Wagner G (2009) A double TROSY hNCAnH experiment for efficient assignment of large and challenging proteins. J Am Chem Soc 131:12880–12881

Ghosh D, Mondal M, Mohite GM, Singh PK, Ranjan P, Anoop A, Ghosh S, Jha NN, Kumar A, Maji SK (2013) The Parkinson's disease-associated H50Q mutation accelerates α-synuclein aggregation in vitro. Biochemistry 52:6925–6927

Grzesiek S, Anglister J, Ren H, Bax A (1993) Carbon-13 line narrowing by deuterium decoupling in deuterium/carbon-13/nitrogen-15 enriched proteins. Application to triple resonance 4D J connectivity of sequential amides. J Am Chem Soc 115:4369–4370

Hiller S, Fiorito F, Wuthrich K, Wider G (2005) Automated projection spectroscopy (APSY). Proc Natl Acad Sci USA 102:10876–10881

Hoch JC, Stern AS (2001) Maximum entropy reconstruction, spectrum analysis and deconvolution in multidimensional nuclear magnetic resonance. NMR Biol Macromol Pt A 338:159–178

Isaksson L, Mayzel M, Saline M, Pedersen A, Rosenlow J, Brutscher B, Karlsson BG, Orekhov VY (2013) Highly efficient NMR assignment of intrinsically disordered proteins: application to B- and T cell receptor domains. PLoS ONE 8:e62947

Jaravine V, Ibraghimov I, Orekhov VY (2006) Removal of a time barrier for high-resolution multidimensional NMR spectroscopy. Nat Methods 3:605–607

Kang L, Janowska MK, Moriarty GM, Baum J (2013) Mechanistic insight into the relationship between N-terminal acetylation of α-synuclein and fibril formation rates by NMR and fluorescence. PLoS ONE 8:e75018

Kazimierczuk K, Zawadzka A, Kozminski W, Zhukov I (2006) Random sampling of evolution time space and Fourier transform processing. J Biomol NMR 36:157–168

Keller R (2004) Optimizing the process of nuclear magnetic resonance spectrum analysis and computer aided resonance assignment. In CANTINA, Verlag, Goldau, Switzerland. Swiss Federal Institute of Technology Zurich, Switzerland

Korzhnev DM, Ibraghimov IV, Billeter M, Orekhov VY (2001) MUNIN: application of three-way decomposition to the analysis of heteronuclear NMR relaxation data. J Biomol NMR 21:263–268

Kosol S, Contreras-Martos S, Cedeño C, Tompa P (2013) Structural characterization of intrinsically disordered proteins by NMR spectroscopy. Molecules 18:10802–10828

Kragelj J, Ozenne V, Blackledge M, Jensen MR (2013) Conformational propensities of intrinsically disordered proteins from NMR chemical shifts. ChemPhysChem 14:3034–3045

Kumar D (2013a) Reduced dimensionality (4,3)D-hnCOCANH experiment: an efficient backbone assignment tool for NMR studies of proteins. J Struct Funct Genom 14:109–118

Kumar D (2013b) Reduced dimensionality tailored HN(C)N experiments for facile backbone resonance assignment of proteins through unambiguous identification of sequential HSQC peaks. J Magn Reson 237:85–91

Kumar D, Paul S, Hosur RV (2010a) BEST-HNN and 2D (HN)NH experiments for rapid backbone assignment in proteins (vol 204, pp 111, 2010). J Magn Reson 207:173–174

Kumar D, Reddy JG, Hosur RV (2010b) hnCOcaNH and hncoCANH pulse sequences for rapid and unambiguous backbone assignment in (13C, 15 N) labeled proteins. J Magn Reson 206:134–138

Liu X, Yang D (2013) HN(CA)N and HN(COCA)N experiments for assignment of large disordered proteins. J Biomol NMR 57:83–89

Löhr F, Rüterjans H (1995) A new triple-resonance experiment for the sequential assignment of backbone resonances in proteins. J Biomol NMR 6:189–197

Mantylahti S, Aitio O, Hellman M, Permi P (2010) HA-detected experiments for the backbone assignment of intrinsically disordered proteins. J Biomol NMR 47:171–181

Mantylahti S, Hellman M, Permi P (2011) Extension of the HA-detection based approach: (HCA)CON(CA)H and (HCA)NCO(-CA)H experiments for the main-chain assignment of intrinsically disordered proteins. J Biomol NMR 49:99–109

Marion D, Ikura M, Tschudin R, Bax A (1989) Rapid recording of 2D NMR spectra without phase cycling. Application to the study of hydrogen exchange in proteins. J Magn Reson 85:393–399

Motackova V, Novacek J, Zawadzka-Kazimierczuk A, Kazimierczuk K, Zidek L, Anderova HS, Krasny L, Kozminski W, Sklenar V (2010) Strategy for complete NMR assignment of disordered proteins with highly repetitive sequences based on resolution-enhanced 5D experiments. J Biomol NMR 48:169–177

Mukrasch MD, Bibow S, Korukottu J, Jeganathan S, Biernat J, Griesinger C, Mandelkow E, Zweckstetter M (2009) Structural polymorphism of 441-residue tau at single residue resolution. PLoS Biol 7:e1000034

Panchal SC, Bhavesh NS, Hosur RV (2001) Improved 3D triple resonance experiments, HNN and HN(C)N, for HN and 15 N sequential correlations in (13C, 15 N) labeled proteins: application to unfolded proteins. J Biomol NMR 20:135–147

Permi P, Hellman M (2012) Alpha proton detection based backbone assignment of intrinsically disordered proteins. In: Uversky VN, Dunker AK (eds) Intrinsically disordered protein analysis. Humana Press, New York, pp 211–226

Piotto M, Saudek V, Sklenář V (1992) Gradient-tailored excitation for single-quantum NMR spectroscopy of aqueous solutions. J Biomol NMR 2:661–665

Rao JN, Kim YE, Park LS, Ulmer TS (2009) Effect of pseudorepeat rearrangement on α-synuclein misfolding, vesicle binding, and micelle binding. J Mol Biol 390:516–529

Reddy JG, Hosur RV (2012) Reduced dimensionality (4,3)D-HN(C)NH for rapid assignment of 1H(N)-15 N HSQC peaks in proteins: an analytical tool for protein folding, proteomics, and drug discovery programs. Anal Chem 84:10404–10410

Rout MK, Mishra P, Atreya HS, Hosur RV (2012) Reduced dimensionality 3D HNCAN for unambiguous HN, CA and N assignment in proteins. J Magn Reson 216:161–168

Rovnyak D, Frueh DP, Sastry M, Sun Z-YJ, Stern AS, Hoch JC, Wagner G (2004) Accelerated acquisition of high resolution triple-resonance spectra using non-uniform sampling and maximum entropy reconstruction. J Magn Reson 170:15–21

Schmieder P, Stern A, Wagner G, Hoch J (1993) Application of nonlinear sampling schemes to COSY-type spectra. J Biomol NMR 3:569–576

Serber Z, Richter C, Dötsch V (2001) Carbon-detected NMR experiments to investigate structure and dynamics of biological macromolecules. ChemBioChem 2:247–251

Shaka AJ, Keeler J, Frenkiel T, Freeman R (1983) An improved sequence for broadband decoupling: WALTZ-16. J Magn Reson 52:335–338

Shaka AJ, Barker PB, Freeman R (1985) Computer-optimized decoupling scheme for wideband applications and low-level operation. J Magn Reson 64:547–552

Sun ZY, Frueh DP, Selenko P, Hoch JC, Wagner G (2005) Fast assignment of 15 N-HSQC peaks using high-resolution 3D HNcocaNH experiments with non-uniform sampling. J Biomol NMR 33:43–50

Szyperski T, Wider G, Bushweller JH, Wuethrich K (1993) Reduced dimensionality in triple-resonance NMR experiments. J Am Chem Soc 115:9307–9308

Szyperski T, Yeh DC, Sukumaran DK, Moseley HNB, Montelione GT (2002) Reduced-dimensionality NMR spectroscopy for high-throughput protein resonance assignment. Proc Natl Acad Sci USA 99:8009–8014

Ulrich EL, Akutsu H, Doreleijers JF, Harano Y, Ioannidis YE, Lin J, Livny M, Mading S, Maziuk D, Miller Z, Nakatani E, Schulte CF, Tolmie DE, Kent Wenger R, Yao H, Markley JL (2008) BioMagResBank. Nucleic Acids Res 36:D402–D408

Wu K-P, Baum J (2011) Backbone assignment and dynamics of human α-synuclein in viscous 2 M glucose solution. Biomol NMR Assign 5:43–46

Zhang SM, Gorenstein DG (2002) Design of Bloch-Siegert phase-shift self-compensated pulses for HCN triple-resonance experiments. Chem Phys Lett 362:278–284